



Effects of absorption coefficients and intermediate-band filling in InAs/GaAs quantum dot solar cells

Hu, Weiguo

Inoue, T.

Kojima, Osamu

Kita, Takashi

(Citation)

APPLIED PHYSICS LETTERS, 97(19):193106-193106

(Issue Date)

2010-11-08

(Resource Type)

journal article

(Version)

Version of Record

(URL)

<https://hdl.handle.net/20.500.14094/90001270>



Effects of absorption coefficients and intermediate-band filling in InAs/GaAs quantum dot solar cells

W. G. Hu,^{1,a)} T. Inoue,² O. Kojima,^{1,2} and T. Kita^{1,2}

¹CREATE, Kobe University, Kobe 657-8501, Japan

²Graduate School of Engineering, Kobe University, Kobe 657-8501, Japan

(Received 7 October 2010; accepted 25 October 2010; published online 10 November 2010)

The effects of absorption coefficients were incorporated in a detailed balance model to analyze the intermediate-band (IB) configuration in quantum dot (QD) solar cells. Our results show that the optimum IB level, E_{IB} , depends on the ratio of two subbandgap absorption coefficient constants, $\alpha_{IC0}/\alpha_{VT0}$. Efficiency contour plots have been calculated to determine the optimum values of E_{IB} and $\alpha_{IC0}/\alpha_{VT0}$. In many cases, a large α_{IC0} results in high conversion efficiency, especially for thin QD solar cells. Optimizing QD shape and size is a promising method to increase α_{IC0} . Increasing the QD total thickness partially addresses the urgent demand for a large α_{IC0} . © 2010 American Institute of Physics. [doi:10.1063/1.3516468]

It has been hypothesized that the efficiency of an intermediate-band (IB) solar cell can exceed the Shockley–Queisser efficiency limit.¹ In this device, two additional subbandgap absorptions—from valence band (VB) to IB and from IB to conduction band (CB)—produce extra photocurrent without degrading the photovoltage. The limiting efficiency is 63.1%, which is far higher than that of a single gap solar cell and slightly higher than that of a two-terminal tandem cell.^{1,2}

The conversion efficiency strongly depends on the IB configuration. Several groups have conducted in-depth studies to optimize this configuration using the detailed balance model. Okada *et al.*³ calculated the efficiency contour plots to determine the appropriate IB level and a suitable material system. For example, without concentration, the maximum efficiency is achieved at 1.5 eV IB level (E_{IB}) and 2.4 eV bandgap (E_g). In the InAs/Ga(N)As quantum dots (QDs) ($E_g = 1.3$ eV) suggested by them, the optimum IB level is 0.9 eV, whereas in common InAs/GaAs QDs ($E_g = 1.42$ eV), the optimum IB level is approximately 0.95 eV. Bremner *et al.*⁴ studied this IB configuration under terrestrial spectrum (AM1.5G, AM1.5D) instead of employing the conventional blackbody approximation. The striking feature of their efficiency contour plot is the presence of multiple maxima. In addition, the IB configuration has been previously discussed under a kind of spectrally selective reflector.⁵ The abovementioned detailed balanced models assume full absorption and an ideal flat-band model. These assumptions are too ideal for designing a real device structure. Moreover, working under these assumptions will result in the factors of absorption and charge spatial distribution not being taken into account; hence, the determined optimum IB level will only depend on the material system used.

InAs/GaAs QD is a promising system for the realization of IB solar cells and many groups have used it to fabricate prototype cells.^{6–11} Although the conversion efficiencies of these devices have not yet exceeded that of the GaAs solar cell, the core process of subbandgap absorptions has been experimentally proved. To overcome the present efficiency

bottleneck, detailed models that account for the absorption process and the energy-band structure need to be developed to guide device design. The purpose of this study is to investigate the effects of absorption coefficients on the IB configuration in InAs/GaAs QD solar cells. In our simulation, we have carefully treated the energy-band structure with the one-dimensional Poisson equation and the continuity equations instead of using flat-band approximation.

The core process of an IB solar cell comprises of a two-step transition: on absorbing one subbandgap photon, an electron transits from VB to IB, and on absorbing another subbandgap photon, the electron in IB is further pumped to CB. IB is electrically isolated from the external circuit; therefore, under the steady state, all the charges in IB are provided by the subbandgap photon absorption-recombination processes. Due to the finite state density of IB, the net-generation rates (VB→IB and IB→CB) have to reach a balance,

$$G_{VI}(x) - R_{VI}(x) = G_{IC}(x) - R_{IC}(x), \quad (1)$$

where G_{ij} is the generation rate and R_{ij} is the radiative recombination rate. In a QD solar cell, the IB energy bandwidth is finite, which results in high effective mass and low electron mobility. Thus, this net-generation balance equation must be satisfied at every position, x .

Upon incorporating the effects of subbandgap absorption coefficients, the generation-recombination processes are represented by¹²

$$G_{ij} = \int \int \alpha_{ij} F_0 \exp(-\alpha_{ij}x) dE dx, \\ R_{ij} = \frac{8\pi}{h^3 c^2} \int \int \alpha_{ij} E^2 \exp\left(-\frac{E}{kT}\right) \exp\left[\left(\frac{\epsilon_{ij}}{kT}\right) - 1\right] dE dx, \quad (2)$$

where α_{ij} is the effective absorption coefficient, F_0 is the photon flux calculated using the Planck formula, and ϵ_{ij} is the quasi-Fermi level splits. In this paper, a 6000 K blackbody is used to simulate solar light at the maximum concentration. It is important to note that the subbandgap absorp-

^{a)}Electronic mail: weiguohu09@gmail.com.

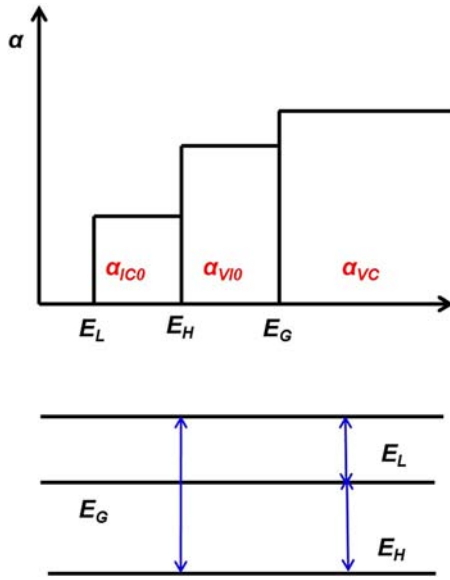


FIG. 1. (Color online) Simplified illustration of absorption coefficient vs photon energy.

tions via IB depend on the probability of IB occupation, which is represented by^{13,14}

$$\alpha_{IC} = f_{IB} \alpha_{IC0}, \quad \alpha_{VI} = (1 - f_{IB}) \alpha_{VI0}, \quad (3)$$

where α_{IC0} and α_{VI0} are the absorption coefficient constants and f_{IB} is the IB occupation possibility that follows the Fermi distribution.

Combining Eq. (1) with the one-dimensional Poisson equation and the continuity equations, we can compute the IB occupation possibility, energy diagram, and, eventually, the conversion efficiency. For a detailed description, refer to Ref. 15. This study focused on the absorption process and assumed the collection efficiency of photocarriers to be 1.

The absorption coefficient constants (α_{IC0} and α_{VI0}) are determined from the oscillator strength and the state density but are independent of the probability of IB occupation. In physics, α_{IC0} and α_{VI0} represent the absorption coefficient when IB is completely full and completely empty, respectively. Until now, very few researchers have reported on experimental or theoretical values for α_{IC0} and α_{VI0} . Birkedal *et al.*¹⁶ measured the 1170 cm^{-1} absorption coefficient (α_{IC}) for a single InAs/GaAs QD, and Zhang and Galbraith¹⁷ calculated intraband absorption coefficients (α_{IC}) of InAs/GaAs QDs to be about $(1-4) \times 10^4 \text{ cm}^{-1}$, subject to the QD geometrical size. Hence, it can be hypothesized that the values of the absorption coefficient constants, α_{IC0} and α_{VI0} , can be on the order of 10^4 cm^{-1} . Figure 1 is a simplified illustration of the absorption coefficient constants. For the sake of simplicity, we adopt the average absorption coefficient constant to describe the absorption processes.

We consider a case wherein subbandgap absorptions are equal to the GaAs absorption, and the total thickness of QDs (W) is 100 nm. Equations (2) and (3) reveal that photocarrier distribution depends on f_{IB} , which is determined by the separate IB quasi-Fermi level, $E_{f_{IB}}$. Figure 2 shows the energy diagram for the QD region, the net-generation rate, and the probability of IB occupation. Our results reveal that the QD state density is not sufficiently high to pin the $E_{f_{IB}}$ at the IB level. $E_{f_{IB}}$ is approximately parallel to the IB level, and f_{IB} depends to a small extent on the spatial position. One of the

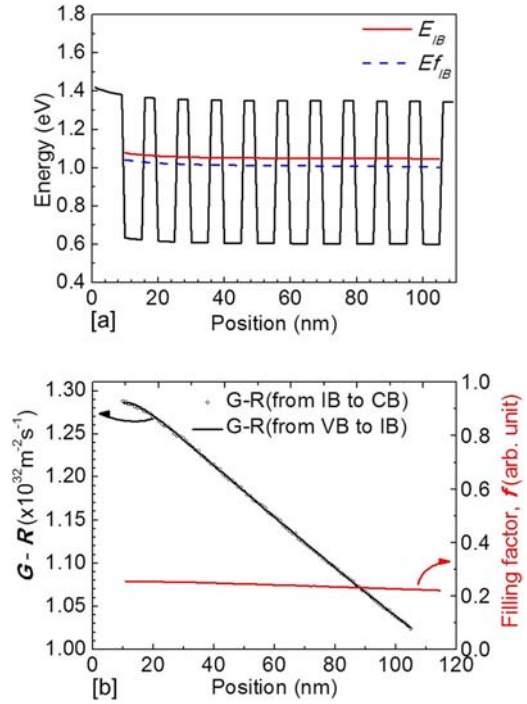


FIG. 2. (Color online) (a) Energy band diagram at maximum power point. (b) Net-generation rate and probability of IB occupation.

important reasons for this is that light intensity decays with penetration depth. The net-generation rates clearly reveal this decay process. Because effective absorption coefficients depend on f_{IB} , they do not follow a simple exponential distribution. The ideal flat-band model assumption, which, among other things, implies that $E_{f_{IB}}$ and f_{IB} remain constant, has been used in many theoretical studies.¹⁻⁵ As a rough approximation, this model is acceptable for solar cells with a thin QD region and uniform absorption coefficients. In addition, the net-generation rate curves of the two subbandgap transitions almost overlap each other, indicating that our numerical resolutions are accurate and stable.

Until now, because of the difficulties in growth technology, most prototype cells only have about 10 InAs/GaAs QD layers ($W < 100 \text{ nm}$). Figure 3(a) shows the efficiency contour plots of 100 nm InAs/GaAs QD solar cells under maximum concentration. Our results reveal that there is no defined value for optimized E_{IB} in any material system; the optimized E_{IB} depends on the ratio of subbandgap absorption coefficient constants, $\alpha_{IC0}/\alpha_{VI0}$. For example, when $\alpha_{IC0}/\alpha_{VI0}$ is increased from 0.1 to 10, the optimized E_{IB} shifts from 1.15 to 0.925 eV. If the spatial dependence of the energy band is neglected, it is easy to understand this tendency. When $\alpha_{IC0}/\alpha_{VI0}$ is decreased, increasing the IB levels increases the photon flux from IB to CB and decreases the photon flux from VB to IB, eventually compensating for the decrease in $\alpha_{IC0}/\alpha_{VI0}$. Similarly, when $\alpha_{IC0}/\alpha_{VI0}$ is increased, optimum IB will shift in the opposite direction. In this structure, the peak efficiency is 45.3% when $\alpha_{IC0}/\alpha_{VI0}$ is 7.9 and E_{IB} is 0.925 eV. Overall, a large α_{IC0} is necessary for high conversion efficiency. Recent studies reveal that optimizing the QD shape and size can relax the selective rule to enhance α_{IC0} .¹⁷ Our efficiency contour plots serve as a reference for the selection of appropriate values for α_{IC0} and E_{IB} .

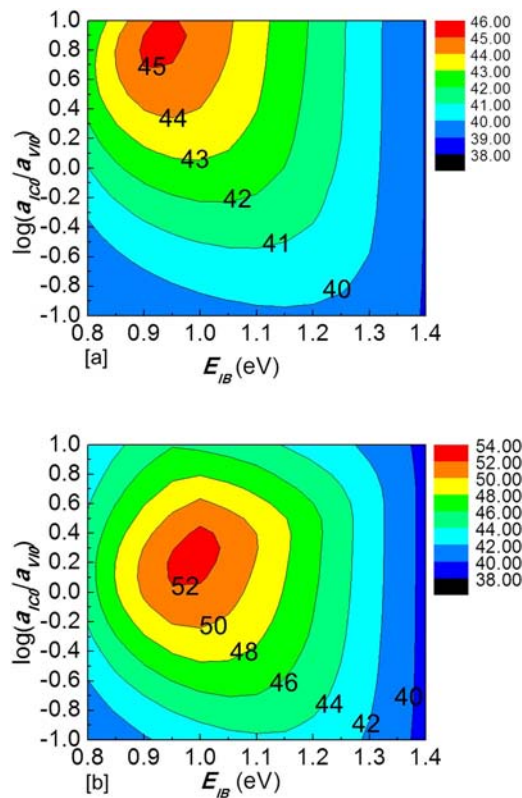


FIG. 3. (Color online) Efficiency contour plots (a) in 100 nm InAs/GaAs QD solar cells and (b) in 500 nm InAs/GaAs QD solar cells.

Recently, Okada *et al.*⁸ adopted the stress-compensation layer technology to grow 50 layer QDs. We simulated a 500 nm InAs/GaAs QD solar cell; its efficiency contour plots are shown in Fig. 3(b). In such thick QD solar cells, the optimum IB level depends on $\alpha_{IC0}/\alpha_{VI0}$; however, the magnitude of shift decreases. If we only consider the increase in incident light decay with increasing W , the absorption efficiency will gradually approach 1; hence, the generation rate will depend to a greater extent on the incident subbandgap photon flux until, eventually, in an infinitely thick QD solar cell, the optimized IB level becomes independent of $\alpha_{IC0}/\alpha_{VI0}$. The peak efficiency reaches 52.8% when $\alpha_{IC0}/\alpha_{VI0}$ and E_{IB} shift to 2.0 and 1.0 eV, respectively. Overall, a large α_{IC0} also results in high conversion efficiency. In addition, increasing W can partially address the urgent demand for a large α_{IC0} .

In the above discussion, we consider α_{VI0} to be equal to α_{VC} . Obviously, α_{VC} only determines the baseline conversion efficiency but does not affect the optimum IB level. The subbandgap absorption is determined by the product of the absorption coefficient (α) and W . Therefore, decreasing α_{VI0}

has an effect similar to that when W is decreased.

In summary, we have studied the effects of absorption coefficients on the probability of IB occupation and configuration. The QD state density is not high enough to pin the $E_{f_{IB}}$ at the IB level. $E_{f_{IB}}$ is approximately parallel to the IB level, and f_{IB} depends to a small extent on the spatial position. The optimum IB level depends on the ratio of two subbandgap absorption coefficient constants, $\alpha_{IC0}/\alpha_{VI0}$. In 500 nm InAs/GaAs QD solar cells, the peak efficiency is 52.8% when $\alpha_{IC0}/\alpha_{VI0}$ and E_{IB} are 2.0 and 1.0 eV, respectively. Overall, a large α_{IC0} results in high conversion efficiency, which is especially necessary for thin QD solar cell. Optimizing the QD shape and size is a promising method to increase α_{IC0} . Increasing W can partially address the urgent demand for a large α_{IC0} . In addition, efficiency contour plots can be used to choose appropriate $\alpha_{IC0}/\alpha_{VI0}$ and E_{IB} . This study mainly focuses on the InAs/GaAs QDs. If the appropriate material parameters are incorporated, this model can also be applied to other systems.

The authors would like to thank Y. Okada and K. Yoshida for helpful discussions. This work was supported by the Inc. Administrative Agency New Energy and Industrial Technology Development Organization (NEDO), and Ministry of Economy, Trade and Industry (METI), Japan.

¹A. Luque and A. Martí, *Phys. Rev. Lett.* **78**, 5014 (1997).

²A. Martí, E. Antolín, C. R. Stanley, C. D. Farmer, N. López, P. Díaz, E. Cánovas, P. G. Linares, and A. Luque, *Phys. Rev. Lett.* **97**, 247701 (2006).

³Y. Okada, S. Yagi, and R. Oshima, *Oyo Buturi* **79**, 0206 (2010).

⁴S. P. Bremner, M. Y. Levy, and C. B. Honsberg, *Appl. Phys. Lett.* **92**, 171110 (2008).

⁵R. Strandberg and T. W. Reenaas, *Appl. Phys. Lett.* **97**, 031910 (2010).

⁶R. Oshima, A. Takata, and Y. Okada, *Appl. Phys. Lett.* **93**, 083111 (2008).

⁷Y. Okada, R. Oshima, and A. Takata, *J. Appl. Phys.* **106**, 024306 (2009).

⁸R. Oshima, A. Takata, Y. Shoji, K. Akahane, and Y. Okada, "Growth of multi-stacked InAs/GaNAs quantum dots grown with As₂ source in atomic hydrogen-assisted molecular beam epitaxy," *Physica E (Amsterdam)* (in press).

⁹D. Zhou, P. E. Vullum, G. Sharma, S. F. Thomassen, R. Holmestad, T. W. Reenaas, and B. O. Fimland, *Appl. Phys. Lett.* **96**, 083108 (2010).

¹⁰C. O. McPheeters, C. J. Hill, S. H. Lim, D. Derkacs, D. Z. Ting, and E. T. Yu, *J. Appl. Phys.* **106**, 056101 (2009).

¹¹S. M. Hubbard, C. D. Cress, C. G. Bailey, R. P. Raffaele, S. G. Bailey, and D. M. Wilt, *Appl. Phys. Lett.* **92**, 123512 (2008).

¹²A. Martí, L. Cuadra, and A. Luque, *IEEE Trans. Electron Devices* **49**, 1632 (2002).

¹³A. S. Lin, W. Wang, and J. D. Phillips, *J. Appl. Phys.* **105**, 064512 (2009).

¹⁴K. Yoshida, Y. Okada, and N. Sano, *Appl. Phys. Lett.* **97**, 133503 (2010).

¹⁵W. G. Hu, T. Inoue, O. Kojima, and T. Kita, "Energy band structure and the half-filling of the intermediate band in the quantum-dot solar cell," *Phys. Status Solidi C* (to be published).

¹⁶D. Birkedal, J. Bloch, J. Shah, L. N. Pfeiffer, and K. West, *Appl. Phys. Lett.* **77**, 2201 (2000).

¹⁷J.-Z. Zhang and I. Galbraith, *Appl. Phys. Lett.* **84**, 1934 (2004).